Applied Surface Science 351 (2015) 135–139

Contents lists available at ScienceDirect

Applied Surface Science

journal homepage: www.elsevier.com/locate/apsusc

Femtosecond laser-induced periodic surface nanostructuring of sputtered platinum thin films

Ainara Rodríguez[a,b,*], Maria Carmen Morant-Miñana[a,b], Antonio Dias-Ponte[a,b], Miguel Martínez-Calderón[a,b], Mikel Gómez-Aranzadi[a,b], Santiago M. Olaizola[a,b]

[a] CIC microGUNE, Goiru Kalea 9 Polo Innovación Garaia, 20500 Arrasate-Mondragón, Spain
[b] CEIT-IK4 & Tecnun (University of Navarra), Paseo Manuel Lardizábal 15, 20018 San Sebastián, Spain

ARTICLE INFO

Article history:
Received 9 January 2015
Received in revised form 10 April 2015
Accepted 19 May 2015
Available online 29 May 2015

Keywords:
Femtosecond laser
Platinum
Thin film
LIPSS
Nanostructure
2D-FFT

ABSTRACT

In this work, submicro and nanostructures self-formed on the surface of Platinum thin films under femtosecond laser-pulse irradiation are investigated. A Ti:Sapphire laser system was used to linearly scan 15 mm lines with 100 fs pulses at a central wavelength of 800 nm with a 1 kHz repetition rate. The resulting structures were characterized by scanning electron microscopy (SEM) and 2D-Fast Fourier Transform (2D-FFT) analysis. This analysis of images revealed different types of structures depending on the laser irradiation parameters: random nanostructures, low spatial frequency LIPSS (LSFL) with a periodicity from about 450 to 600 nm, and high spatial frequency LIPSS (HSFL) with a periodicity from about 80 to 200 nm. Two different modifications regimes have been established for the formation of nanostructures: (a) a high-fluence regime in which random nanostructures and LSFL are obtained and (b) a low-fluence regime in which HSFL and LSFL are obtained.

1. Introduction

In the last decade, Laser-Induced Periodic Surface Structures (LIPSS) have attracted increased research attention because of their applications in surface hydrophobic/hydrophilic properties [1], friction reduction [2,3], control of the surface reflection [4], control of the cell growth direction [5], or Surface-Enhanced Raman Spectroscopy [6]. LIPSS have been induced in a wide variety of materials by pulsed lasers in the nanosecond (ns) to femtosecond (fs) regimes [3,7–20]. Two distinct types of LIPSS have been identified so far: Low Spatial Frequency LIPSS (LSFL) and High Spatial Frequency LIPSS (HSFL). Their orientations can be either parallel or perpendicular to the incident laser beam polarization, depending both on laser irradiation parameters and material properties [12,19]. LSFL have a spatial period close to or slightly smaller than the irradiation laser wavelength. Their formation is considered a result of the interference between the incident laser beam and surface-scattered waves [21,22] or Surface Plasmon Polaritons (SPP) [15,23]. HSFL have a spatial period that is much smaller than the laser wavelength. Several theories have been proposed for HSFL formation mechanisms: second harmonic generation (SHG) [10,12,24], self-organization [25], or interference with modification of the optical properties during laser processing [26]. However, none of these theories gives a complete explanation of LIPSS formation; their formation is still debated. Consequently, further investigations on the resulting LIPSS on different materials and under different irradiation conditions can help to better understand their formation mechanism. LIPSS have generally been identified in the femtosecond laser regime on bulk materials, semiconductors [11,15], dielectrics [17,27] and metals [16,23,27–30]. Among metallic materials, platinum is of particular interest due to its use as contact electrode in microsensing applications or as chemical catalyst, where high surface-to-volume ratio may lead to an increased sensitivity and/or enhanced performance [23]. The formation of LIPSS on bulk platinum has been already studied by other groups [23,28–30]. These authors have reported LSFL perpendicularly oriented to the laser beam polarization with periods varying from 0.55 to 0.69 μm depending on the irradiation conditions. Table 1 provides a summary of the obtained LIPSS on this material, which includes the most relevant process parameters and the period and orientation of the resulting structures.

LIPSS formation on thin metal films instead has been less explored, although is getting increased interest in recent years [20,31,32]. The work here presented is centered on the experimental observation of LIPSS in Pt thin films under ultrafast laser pulses.

* Corresponding author. Tel.: +34 943212800.
E-mail address: airodriguez@ceit.es (A. Rodríguez).

http://dx.doi.org/10.1016/j.apsusc.2015.05.117
0169-4332/

Table 1
Literature review of LIPSS reported on bulk platinum surfaces (λ=790–800 nm, τ = 95–160 fs, f = 1 kHz) at normal incidence in air. Orientation is indicated with respect to laser beam polarization.

Period (nm)	Type	Orientation	Fluence (J cm^{-2})	Number pulses	Reference
620–550	LSFL	⊥	0.084	30–500	[23]
610–560	LSFL	⊥	0.170	30–200	[28]
620–690	LSFL	⊥	0.179–0.421	50	[29]
560	LSFL	⊥	0.220	1000	[30]

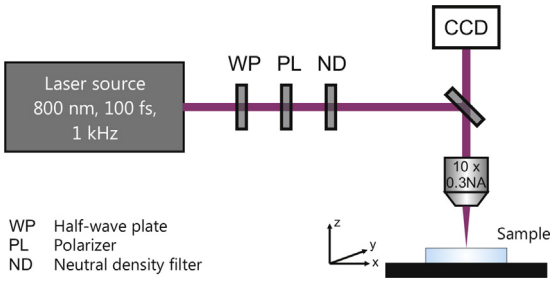

Fig. 1. Schematic layout of the femtosecond laser micro/naomachining setup.

2. Experimental

2.1. Micro-nanomachining setup

A direct-write femtosecond laser micro-nanomachining tool was used for LIPSS experiments. A laser system consisting of a Ti:Sapphire mode-locked oscillator and a regenerative amplifier was used to generate 100 fs pulses at a central wavelength of 800 nm with a 1 kHz repetition rate. The pulse energy was adjusted with a two step setup: a constant attenuator consisting of several neutral density filters and a variable attenuator formed by a half-wave plate and a low dispersion polarizer. The 12 mm-diameter laser beam was focused on the sample using a 10x microscope objective with a NA of 0.3. This objective, together with a CCD camera, was used for online monitoring of the structuring process. The layout of the experimental setup is shown in Fig. 1.

2.2. Fabrication process

The substrate material for all the samples was a 200 nm-thick Pt thin layer deposited by magnetron sputtering onto thermally oxidized 3″ silicon wafers.

Microstripes of 15 mm long were written on the surface of the Pt thin film with a fixed pulse energy of 70 nJ in order to generate the LIPSS. The sample was placed in a motorized XYZ stage, which allowed controlling (1) the number of laser shots applied by varying the scan speed, and (2) the laser fluence by changing the distance between the objective and the sample surface (defocusing distance). This way, samples were irradiated with pulses with Gaussian beam radius of 2.23, 2.49, 3.15, 4.02, 4.99 and 6.01 μm, resulting in laser fluences of 24, 38, 142, 231, 370 and 463 mJ cm^{-2}, respectively.

The number of effective pulses was calculated using Eq. (1) for the range of scanning speeds tested (0.02–0.60 mm s^{-1}),

$$Neff = \frac{D \cdot f}{v} \quad (1)$$

being D the Gaussian beam diameter, f the repetition rate of the laser source and v the scanning speed. Table 2 summarizes the number of effective pulses applied for each processing condition.

Platinum surface nanostructuring took place in air for all experiments. After laser processing, all the samples were ultrasonically cleaned in ethanol for 10 min and subsequently rinsed off in de-ionized water.

Table 2
Number of effective pulses for the whole range of scan speeds tested, calculated using Eq. (1).

Beam radius (μm)	Scan speed (mm s^{-1})						
	0.60	0.30	0.20	0.10	0.06	0.03	0.02
2.23	7	15	22	45	74	149	223
2.49	8	17	25	50	83	166	249
3.15	11	21	32	63	105	210	315
4.02	13	27	40	80	134	268	402
4.99	17	33	50	100	166	333	499
6.01	20	40	60	120	200	401	601

2.3. Characterization

The resulting surface topographies were characterized by field emission scanning electron microscopy (FESEM) and Atomic Force Microscopy (AFM). A free and open source software (Gwyddion) was used to perform the two dimensional Fast Fourier Transform (2D-FFT) of the micrographs. The 2D-FFT provides an effective way to analyze the entire images and gives therefore, more representative values for LIPSS periods than singular values deduced from FE-SEM micrographs.

3. Results

3.1. Effect of laser fluence and number of applied pulses

The most representative topographies obtained with this experimental set-up are shown in Fig. 2. These patterns are characterized by the shape, period (Λ) and orientation with respect to the incident laser beam polarization. Perpendicular LSFL, parallel HSFL and non-periodic nanostructures are found for the range of laser fluence and scan speeds tested.

At fluences of 38 mJ cm^{-2}, a scan speed of 0.1 mm s^{-1} (100 pulses) was required to start surface texturing (Fig. 2a); no evidence of material modification was find for higher speeds. This fluence and scan speed resulted in a set of shallow grooves formed parallel to the incident laser beam polarization (parallel HSFL). These nanostructures are better defined as the scan speed decreases or the number of pulses applied increases, as can be seen in Fig. 2b and in the AFM micrograph in Fig. 3, where the depth of the resulting HSFL approaches the thickness of the Pt film. Further increasing the number of applied pulses gave rise to LSFL with orientation perpendicular to the laser beam polarization (Fig. 2c). Both HSFL and LSFL coexist for a certain range of applied pulses, although LSFL predominance is more pronounced as the number of pulses increases. The structuring process followed this trend until Pt ablation started to be observed (Fig. 2d), which corresponds to 500 pulses.

At higher fluences instead, 370 mJ cm^{-2} for example, first evidences of surface modification occurred for very low number of applied pulses (N = 8) although the obtained structures were not nanoscale periodic structures but randomly distributed nanostructures (Fig. 2e). These nanostructures get also better defined as the number of pulses applied increases (Fig. 2f), similarly to the previous case. Moreover, subwavelength structures with orientation perpendicular to the laser beam polarization (Fig. 2g) are also generated as the number of applied pulses is further increased until complete ablation of the Pt thin film occurs (Fig. 2h).

The rest of the obtained structures follow the trend of these two last modification regimes, as can be seen in Fig. 4. This figure illustrates the type of resulting structures as a function of the laser fluence and the number of applied pulses for the full range of